

Seismic detection of an active subglacial magmatic complex in Marie Byrd Land, Antarctica

Amanda C. Lough^{1*}, Douglas A. Wiens¹, C. Grace Barcheck^{1,2}, Sridhar Anandakrishnan³, Richard C. Aster^{4,5}, Donald D. Blankenship⁶, Audrey D. Huerta⁷, Andrew Nyblade³, Duncan A. Young⁶ and Terry J. Wilson⁸

Numerous volcanoes exist in Marie Byrd Land, a highland region of West Antarctica. High heat flow through the crust in this region may influence the stability of the West Antarctic Ice Sheet^{1–4}. Volcanic activity progressed from north to south in the Executive Committee mountain range between the Miocene and Holocene epochs, but there has been no evidence for recent magmatic activity^{5–7}. Here we use a recently deployed seismic network to show that in 2010 and 2011, two swarms of seismic activity occurred at 25–40 km depth beneath subglacial topographic and magnetic highs, located 55 km south of the youngest subaerial volcano in the Executive Committee Range. We interpret the swarm events as deep long-period earthquakes based on their unusual frequency content. Such earthquakes occur beneath active volcanoes, are caused by deep magmatic activity and, in some cases, precede eruptions^{8–11}. We also use radar profiles to identify a prominent ash layer in the ice overlying the seismic swarm. Located at 1,400 m depth, the ash layer is about 8,000 years old and was probably sourced from the nearby Mount Waesche volcano. Together, these observations provide strong evidence for ongoing magmatic activity and demonstrate that volcanism continues to migrate southwards along the Executive Committee Range. Eruptions at this site are unlikely to penetrate the 1.2 to 2-km-thick overlying ice, but would generate large volumes of melt water that could significantly affect ice stream flow.

Marie Byrd Land (MBL) is a remote continental region that remains poorly understood owing to burial beneath the West Antarctic Ice Sheet (WAIS) and historically limited geological and geophysical data^{6,12}. Extension between East and West Antarctica began with the breakup of Gondwanaland in the Mesozoic era and continued into the Cenozoic era forming the West Antarctic Rift System (WARS) and introducing tensional stress and high heat flow into MBL (ref. 12). Volcanism became widespread during the late Cenozoic and several volcanoes remain active to recent times, as noted by fumarolic activity and ash records^{2,6}. Topographic and aeromagnetic studies suggest Holocene volcanic activity, but until now there has been no direct evidence supporting present MBL magmatism^{2,6,7}.

The International Polar Year POLENET/ANET project, which includes three-component broadband seismic stations deployed across West Antarctica beginning in December 2007, provides

the first large-scale data set that can be used to detect seismic signals resulting from active magmatism in this region. Most of the stations used here were installed in January 2010, comprising two crossing lines of temporary stations with the purpose of studying the structure of the WARS (Fig. 1, Supplementary Table 1.1, Methods).

We used an automated event detection and location algorithm to produce an initial list of seismic sources. Most events define an unusual cluster near 77.65° S, 126.46° W coinciding with a subglacial mountain complex along the southward extension of the Executive Committee Range (ECR; Fig. 1). Using manual picking and detection on a subset of nearby stations, we located 1,370 events in this region showing at least six strong P- or S-phase arrivals, with two to three times more events observable at only the two closest stations (Supplementary Table 1.1). We closely examined a representative sample (5 days of data every 20 days, unless during a seismic swarm) to better track temporal changes in the seismicity rate. Activity persisted throughout the deployment (January 2010–December 2011), with only one month having no detections (Supplementary Fig. 2.1). Most events (nearly 90%) occurred during two swarms in January–February 2010 and March 2011. The first swarm was only partially captured because nearby stations began operating shortly after 17 January. We have no methods of assessing seismicity before POLENET/ANET observations, but the observed seismicity suggests this is a region of persistent activity.

The events are small, most with local magnitudes between M_L 0.8 and 2.1, with a median of 1.44 and a maximum of 3.03. The b -value characterizing the magnitude–frequency relationship is 2.75, which is large relative to tectonic earthquake catalogues, but is consistent with values commonly observed in volcanic earthquake swarms (Supplementary Fig. 2.2; refs 13,14). These magnitude statistics do not reflect the smallest events recorded on only the two closest stations because their locations and magnitudes are more uncertain.

We used relative relocation on a subset of events with eight or more arrivals, removing events with large uncertainties (defined by the average of the three 95% confidence semi-axes lengths) until the greatest uncertainty was 8 km, leaving 203 events (Fig. 1). Relocations were calculated using both the IASP91 global velocity model¹⁵ and a local velocity model (Supplementary Table 1.2) that incorporated the thin crust and low-velocity upper mantle of West Antarctica constrained by POLENET/ANET data¹⁶. We observe no significant difference in hypocenter locations or depth estimates

¹Department of Earth and Planetary Sciences, Washington University, St Louis, Missouri 63130, USA, ²Department of Earth and Planetary Sciences, University of California-Santa Cruz, Santa Cruz, California 95064, USA, ³Department of Geosciences, Pennsylvania State University, University Park, Pennsylvania 16802, USA, ⁴Department of Earth and Environmental Science, New Mexico Tech, Socorro, New Mexico 87801, USA, ⁵Geosciences Department, Colorado State University, Fort Collins, Colorado 80523, USA, ⁶Institute for Geophysics, The University of Texas at Austin, Austin, Texas 78759, USA, ⁷Department of Geological Science, Central Washington University, Ellensburg, Washington 98926, USA, ⁸Department of Geological Sciences, Ohio State University, Columbus, Ohio 43210, USA. *e-mail: alough@levee.wustl.edu

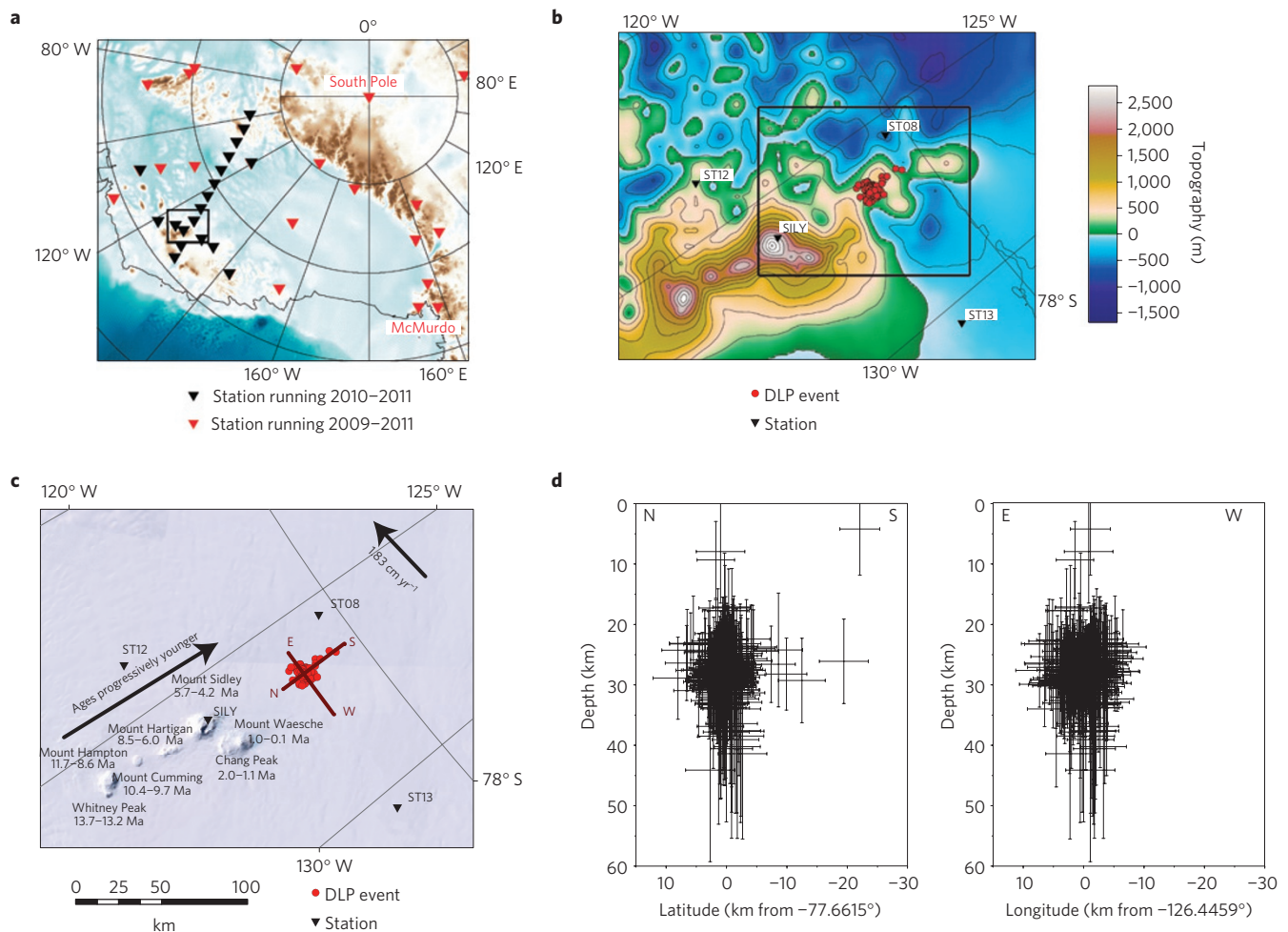


Figure 1 | Summary of ECR volcanic and seismic activity. **a**, POLNET stations over bed topography⁴. **b**, Box in **a** over bed topography with 250 m contours⁴. DLP events occur beneath a subglacial topographic high. The box outlines Fig. 3a,b. **c**, Box in **a** over Landsat Image Mosaic of Antarctica imagery. ECR volcanoes are labelled with dates of known volcanism¹. DLP swarms occur 55–60 km from Mount Sidley along age-progression line. Arrow shows HS3-NUVELA1A plate motions²⁰. Ma, Myr ago. **d**, Depth profiles in north-south (left) and east-west (right) cross-sections showing relocated events. Error bars are average 95% confidence intervals and horizontal errors show average for latitude and longitude.

depending on the model. Relocation collapsed the size of the main cluster to approximately 35% of its original area and located nearly all events to depths of 25–40 km (Fig. 1d; Supplementary Fig. 2.3.1). The depths are robust with respect to perturbations of input, including removal of all S-phases, removal of any individual station and changes to the structure model. Investigation of waveform similarity using a cross-correlation algorithm shows only a mediocre average correlation coefficient of 0.6, demonstrating that these are not repeating events with nearly identical locations and mechanisms. However, swarm events correlate better with each other than the entire data set, with correlation coefficients up to about ~0.8 (Supplementary Fig. 2.4.1, 2.4.2). Thus the cluster comprises a variety of seismic sources that change with time.

In this region, seismic events could conceivably arise from glacial, tectonic, or volcanic processes. The cluster events show an unusual spectral character, with a maximum spectral amplitude at 2–4 Hz, compared with 10–20 Hz expected for tectonic events of this magnitude. This observation, along with the unusual swarm-like behaviour and depth, strongly suggests a non-tectonic origin (Fig. 2; Supplementary Fig. 2.3.2; ref. 17). Glacial processes can generate low-frequency events, however the well-constrained source depths of 25–40 km preclude a glacial origin (Fig. 1d; Supplementary Fig. 2.3.1; ref. 18). These depths place the swarm near the MBL Moho depth¹⁶, deeper than most tectonic seismicity

in comparable regions such as the Basin and Range Province of North America and far below the typical brittle/ductile transition in such regions^{6,12–14}.

The entire data set of 1,370 events shows characteristics consistent with deep long-period (DLP) sources identified in many volcanic settings including the Aleutian Islands, the Pacific Northwest, Hawaii and Mount Pinatubo (Fig. 2; refs 8–11). DLP events are characterized by deep hypocenters (at or below the brittle–ductile transition zone), low-frequency energy (<5 Hz), emergent signals and long codas⁸. In all cases DLPs are associated with active magmatic processes^{8–11} although the physical mechanism producing DLPs is unknown at present. They often show swarm behaviour and are hypothesized to represent movement of magma and other fluids that lead to pressure-induced vibrations in cracks within volcanic and hydrothermal systems⁹. DLP swarms have commonly been associated with other forms of volcanic and magmatic activity, including eruptions and intrusions^{8–11}.

As well as showing the characteristics of DLPs, the cluster occurs where present volcanic activity would be expected along the north–south-migrating volcanic trend in the ECR. It is located beneath a subglacial topographic high ~1,000 m above surrounding low-lying areas extending beyond Mount Sidley in the apparent migration direction of the ECR volcanoes (Figs 1b, 3; Supplementary Fig. 1.3; ref. 4). Geophysical Exploration of Marie

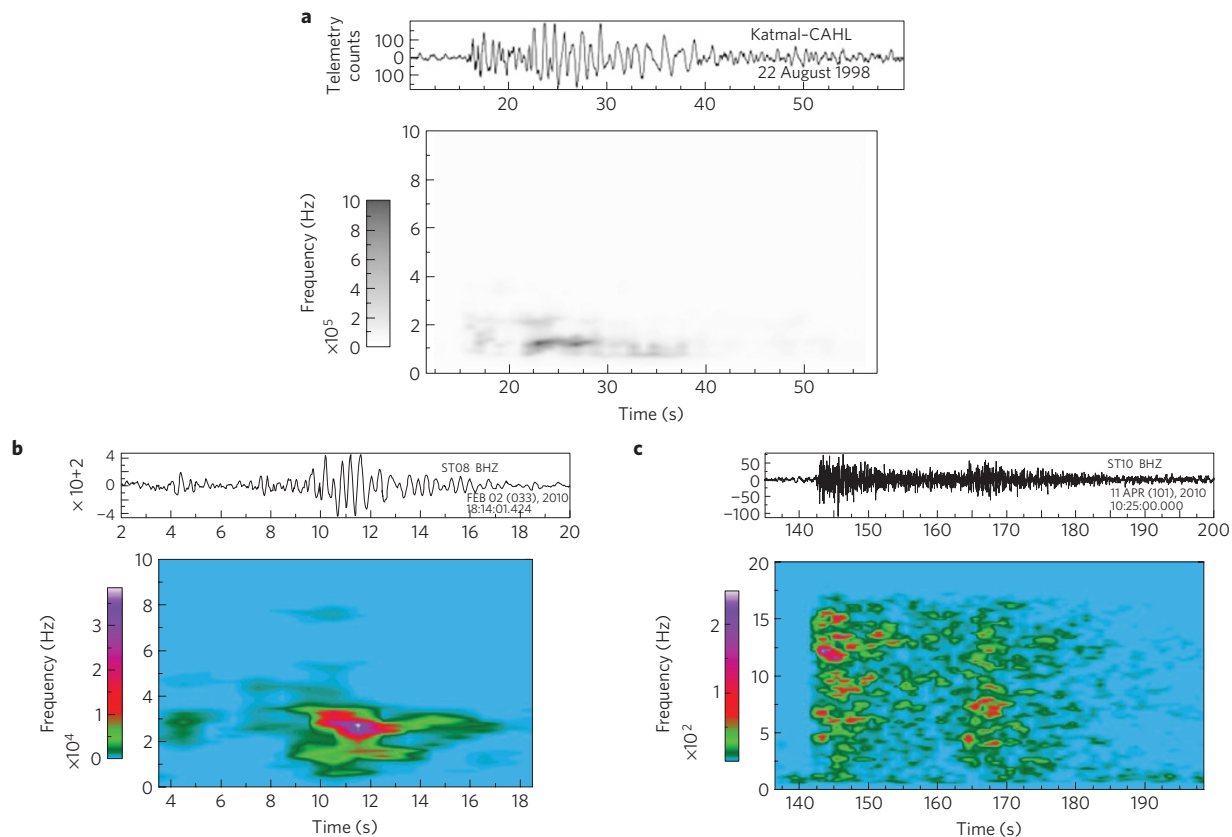


Figure 2 | Comparison of spectral character of DLP and non-DLP events. **a**, Example spectrogram of a DLP from CAHL station on Cahil, Katmai, Alaska in the Aleutian Islands¹⁰. **b**, A spectrogram from a ECR DLP event, magnitude M_L 1.71. Waveform is filtered using a 0.5 Hz four-pole high-pass filter. **c**, A spectrogram from a tectonic (potentially volcano-tectonic) event on Mount Berlin magnitude M_L 2.72. Waveform is filtered using a 0.9 Hz four-pole high-pass filter.

Byrd Land Evolution (GIMBLE) and earlier Airborne Geophysical Survey of Amundsen Embayment (AGASEA; ref. 19) aeromagnetic data reveal a narrow 400 nT anomaly over this high, consistent with local volcanic emplacement (Fig. 3a,b)⁶. Incorporating the oldest known ages for Whitney Peak (13.7 Myr) and Mount Sidley (5.7 Myr) lavas², we calculate a volcanic centre southward migration rate of ~ 9.6 km Myr⁻¹ (Fig. 1c). This predicts that the present centre of volcanism should be approximately 55 km south of Mount Sidley, consistent with the 55–60 km distance of the observed cluster. Interestingly, the migration of volcanism along the ECR is approximately perpendicular to the expected hotspot migration direction from plate motion within the HS2-NUVEL1A hotspot reference frame²⁰, although uncertainties are large for Antarctica (Fig. 1c).

This cluster of events represents a present location of active intraplate magmatic activity along the ECR. The cluster is centred beneath a subglacial mountain complex we interpret as a volcanic edifice, it is in the expected location of present volcanism based on volcanic trends, hypocenters are significantly deeper than for a non-magmatic source, and waveforms and spectra are consistent with DLP events rather than with similarly sized tectonic events.

It is unclear whether the observed DLP swarm activity presages an imminent eruption. Increased DLP activity can precede eruptions (for example, the 1991 Mount Pinatubo eruption)¹¹ but in other cases occurs as part of the background seismicity and thus is not a reliable precursor^{8–10}. We do not believe subglacial volcanic eruptions accompanied the two swarms of increased DLP activity in 2010–2011. Only DLP activity was increased during these swarms and an eruption should produce detectable shallow volcanic seismicity. The deep magmatic activity we observed has

been ongoing for an indeterminate amount of time and has almost certainly accompanied past eruptions, consistent with a volcanic edifice inferred in the subglacial topography (Figs 1b, 3c).

GIMBLE and AGASEA radar data from flights near the ECR show a highly reflective layer 400–1,400 m below the surface, interpreted as volcanic ash, in the ice overlying the cluster location. This layer seems to conform to the local ice stratigraphy, in some cases showing deformation from basal melting (Fig. 3). The layer spans a 50×20 km ellipse, covering 785 km², pointing south in the prevailing wind direction²¹. Ice flow is complex owing to rough topography in this region, which has deformed the layer. Given modern accumulation rates of 12.5 cm yr⁻¹, we estimate using a Dansgaard–Johnsen model the layer age is $\sim 8,000$ years (ref. 22).

The ash layer could result from the volcanic edifice overlying the DLP cluster, but both the observation of tephra bands in a zone of ablating blue ice and the distribution of the layer in a wind-oriented streak south of Mount Waesche suggest the source is most probably Mount Waesche^{23,24}. Perhaps the strongest argument for a Mount Waesche source is the implausibility of an eruption from the DLP source venting ash to the surface. DLPs are known to occur up to 5 km from active vents^{8–11} and the aerogeophysical lines, spaced ~ 15 km apart, approach within 5 km of the DLP source, where ice thickness is $\sim 1,100$ m. Owing to the vent location uncertainties as well as gaps in the radar coverage, the ice thickness over the vent is uncertain; a conservative assumption is that the vent is likely to be covered by at least 1 km of ice. Approximately 6×10^{15} kJ are required to melt a cylinder of ice 5 km in diameter and 1 km thick (Supplementary Information 2.5, Table 2.5). Large eruptions release $\sim 1 \times 10^{17}$ kJ of thermal energy whereas more typical eruptions release of the order of 10^{12} – 10^{13} kJ, suggesting only

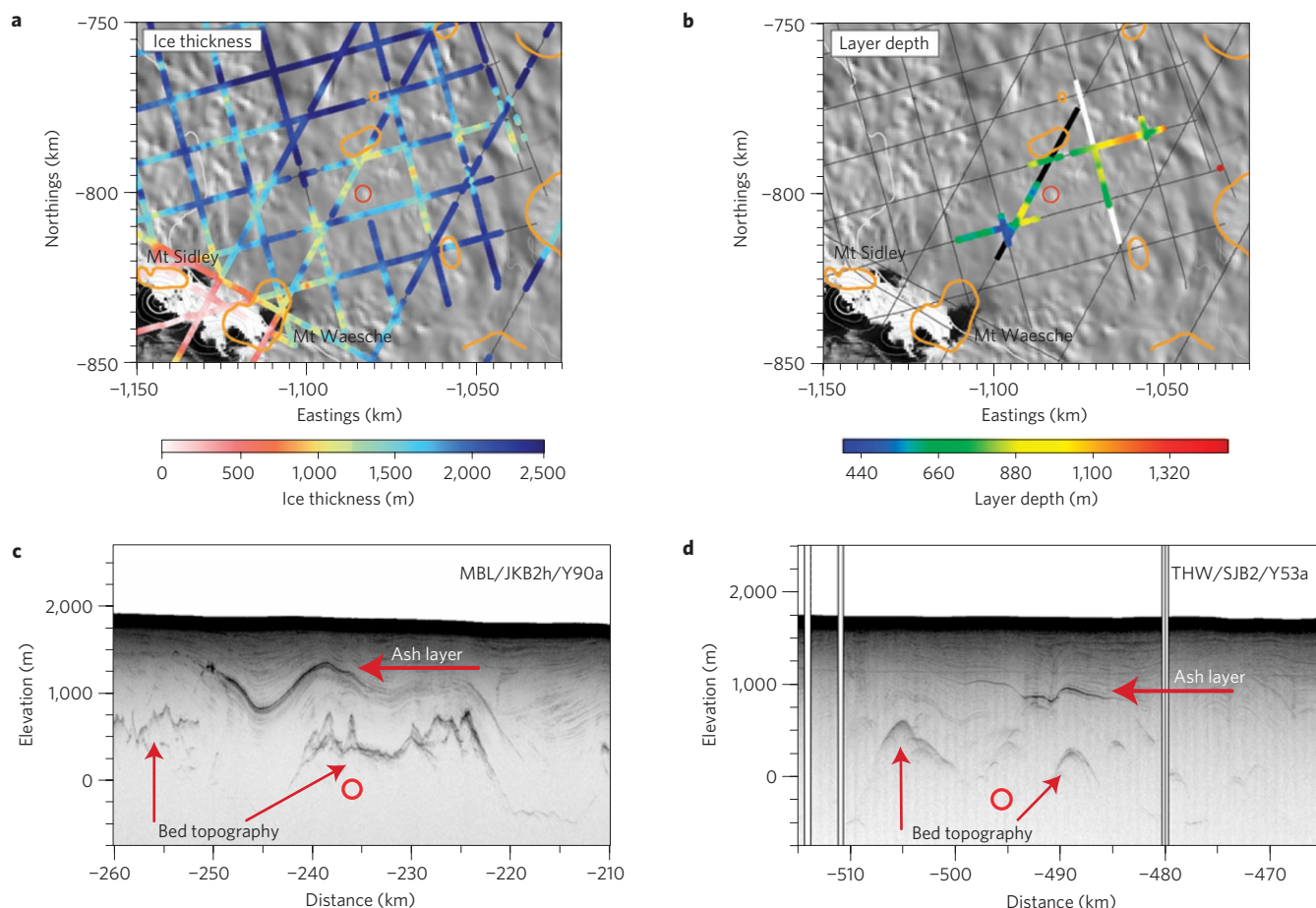


Figure 3 | Radar data showing ice thickness and ash layer. **a**, Box in Fig. 1b showing available radar lines and ice thickness. Red circle is DLP cluster and orange outlines magnetic anomalies ($+100$ nT contours). Plotted over surface imagery³⁰ and elevation contours⁴. **b**, Corresponding map showing depth to ash layer. **c**, Focused GIMBLE profile along thick black line in **b**. Red circle is closest to DLP cluster. Ash closely follows bed topography, leading to a large change in elevation across the profile. A bed topographic low occurs in this location (Fig. 1b). **d**, Unfocused AGASEA profile along thick white line in **b** (ref. 20).

an exceptionally large eruption could breach the ice cap and vent to the surface (Supplementary Information 2.5, Table 2.5; ref. 25).

The discovery of an active subglacial magmatic system in MBL associated with proximal subaerial ash layer deposition from Holocene eruptions highlights the question of the potential impact of the southward migration of the ECR magmatic complex on the WAIS. As active volcanic centres extending from the ECR begin to impact the deeper interior of the WAIS we expect this region to generate larger volumes of melt water at the ice sheet base associated both with subglacial eruptions and increasing background heat flow. Melt water from the extended ECR magmatic complex enters the hydrological catchment of the MacAyeal Ice Stream,²⁶ characterized by a mean annual water flux of 0.63 km^3 . A 10^{13} kJ eruption would melt $\sim 0.035 \text{ km}^3$ of ice (Supplementary Information 2.6), whereas an anomalously large eruption would exceed the annual flux by several orders of magnitude (10^{17} kJ melts $\sim 350 \text{ km}^3$), perhaps in a matter of days. Water flux modulation by such eruptions as well as by the associated increase in background heat flow from magmatic migration will potentially lubricate the bed and increase the velocity of the overlying ice, facilitating the evolution of ice streams and changing rates of ice mass loss in West Antarctica^{3,5–7}.

Methods

Data collection. All seismic data used here were collected as part of the POLENET/ANET seismic deployment, beginning in January 2010 and continuing

to December 2011. Instruments were installed beginning 17 January 2010 and the relevant parts of the array were fully deployed beginning 21 January 2010. Instrumentation consisted of Guralp cold-weather 3T or Nanometrics Trillium T-240 broadband seismographs connected to Quantera Q-330 digitizers enclosed in insulated boxes with Baler-14 or Baler-44 storage drives. Austral summer power was provided by lead-acid batteries recharged by solar panels and wind generators. Austral winter power was provided by either lead-acid or lithium batteries depending on station configuration. Equipment and technical support was provided by IRIS PASSCAL. Three-component data were collected continuously over the instrumentation period at sampling rates of 40 and 1 sample s^{-1} . GIMBLE radar and magnetics data were collected on a DC-3T aircraft using the same instrument set-up as the ICECAP deployment (an aerogeophysical survey supported by Casey Station that gathered data January–December 2008–2009 and 2009–2010; ref. 27). GIMBLE HICARS radar data were focused where possible²⁸.

Data analysis. 40 sample s^{-1} data were organized into a database using the Antelope software package. A preliminary automated short term average/long term average detection was run to identify and locate local seismic events. When we found most DLP events were missed by the automated detection, we manually inspected and picked P- and S-phases for a representative sample of the data. All events with greater than six combined P- and S-arrivals were picked for the January–February 2010 and March 2011 swarms. For the rest of the data period, five-day subsets of data were picked every 20 days. All picked data were located using the dbgenloc module of Antelope. All events with greater than eight combined arrivals were then input into a relative relocation program (following methods outlined in ref. 29) and events with uncertainties (combined 95% confidence interval over latitude, longitude and depth) less than 8 km were used for the final subset of 203 DLP events. Both a local velocity model and the IASP91 global model were used in relocation, reported hypocenters are from the local velocity model calculations¹⁵. We generated and visually inspected spectrograms for all DLP events at ST08 and SILY stations. No DLP spectrograms showed abnormal frequencies at

either ST08 or SILY station. A cross-correlation analysis was carried out on ST08 and SILY stations to assess the similarity of waveforms (Supplementary Figs 3, 4). A dendrogram-based cluster analysis was also carried out on these stations to check the results of the cross-correlation analysis.

Received 11 June 2013; accepted 26 September 2013;
published online 17 November 2013

References

- Paulsen, T. S. & Wilson, T. J. Evolution of Neogene volcanism and stress patterns in the glaciated West Antarctic Rift, Marie Byrd Land, Antarctica. *J. Geol. Soc. Lond.* **167**, 401–416 (2010).
- LeMasurier, W. E. & Thomson, J. W. (eds) in *Volcanoes of the Antarctic Plate and Southern Oceans* (American Geophysical Union, 1990).
- Blankenship, D. D. *et al.* Active volcanism beneath the West Antarctic ice sheet and implications for ice-sheet stability. *Nature* **361**, 526–529 (1993).
- Fretwell, P. *et al.* Bedmap2: Improved ice bed, surface and thickness datasets for Antarctica. *Cryosphere Discuss.* **6**, 4305–4361 (2012).
- Corr, H. F. & Vaughan, D. G. A recent volcanic eruption beneath the West Antarctic ice sheet. *Nature Geosci.* **1**, 122–125 (2008).
- Behrendt, J. C. The aeromagnetic method as a tool to identify Cenozoic magmatism in the West Antarctic Rift System beneath the West Antarctic Ice Sheet — A review; Thiel subglacial volcano as possible source of the ash layer in the WAISCOPE. *Tectonophysics* **585**, 124–136 (2013).
- Vogel, S. W. *et al.* Geological constraints on the existence and distribution of West Antarctic subglacial volcanism. *Geophys. Res. Lett.* **33**, L23501 (2006).
- Nichols, M. L., Malone, S. D., Moran, S. C., Thelen, W. A. & Vidale, J. E. Deep long-period earthquakes beneath Washington and Oregon volcanoes. *J. Volcanol. Geotherm. Res.* **200**, 116–128 (2011).
- Okubo, P. G. & Wolfe, C. J. Swarms of similar long-period earthquakes in the mantle beneath Mauna Loa Volcano. *J. Volcanol. Geophys. Res.* **178**, 787–794 (2008).
- Power, J. A., Stihler, S. D., White, R. A. & Moran, S. C. Observations of deep long-period (DLP) seismic events beneath Aleutian arc volcanoes; 1989–2002. *J. Volcanol. Geotherm. Res.* **138**, 243–266 (2004).
- White, R. A. in *Fire and Mud: Eruptions and Lahars of Mount Pinatubo, Philippines* (eds Newhall, C. G. & Punongbayan, R. S.) 307–328 (Univ. of Washington Press, 1996).
- Winberry, J. P. & Anandakrishnan, S. Seismicity and neotectonics of West Antarctica. *Geophys. Res. Lett.* **30**, 18,1931 (2003).
- McNutt, S. R. *Monitoring and Mitigation of Volcano Hazards* 99–146 (Springer, 1996).
- Jakobsdóttir, S. S. *et al.* Earthquake swarms at Upptyppingar, north-east Iceland: A sign of magma intrusion? *Stud. Geophys. et Geodaet.* **52**, 513–528 (2008).
- Kennett, B. L. N., Engdahl, E. R. & Buland, R. Constraints on seismic velocities in the Earth from traveltimes. *Geophys. J. Int.* **122**, 108–124 (1995).
- Chaput, J. *et al.* Crustal thickness across West Antarctica. *J. Geophys. Res.* (in review, 2013).
- Abercrombie, R. E. Earthquake scaling relationships from -1 to $5M_L$ using seismograms recorded at 2.5-km depth. *J. Geophys. Res.* **100**, 24015–24036 (1995).
- Zoet, L. K., Anandakrishnan, S., Alley, R. B., Nyblade, A. A. & Wiens, D. A. Motion of an Antarctic glacier by repeated tidally modulated earthquakes. *Nature Geosci.* **5**, 623–626 (2012).
- Holt, J. W. *et al.* New boundary conditions for the West Antarctic ice sheet: Subglacial topography of the Thwaites and Smith Glacier catchments. *Geophys. Res. Lett.* **33**, L09502 (2006).
- Gripp, A. E. & Gordon, R. G. Young tracks of hotspots and current plate velocities. *Geophys. J. Int.* **150**, 321–361 (2002).
- Lenaerts, J. T. M. & Van den Broeke, M. R. Modelling drifting snow in Antarctica with a regional climate model: 2. results. *J. Geophys. Res.* **117**, D05108 (2012).
- Van de Berg, W., Van de Broeke, M., Reijmer, C. & Van Meijgaard, E. Characteristics of the Antarctic surface mass balance, 1958–2002, using a regional atmospheric climate model. *Ann. Glaciol.* **41**, 97–104 (2005).
- Ackert, J. *et al.* Measurements of past ice sheet elevations in interior West Antarctica. *Science* **286**, 276–280 (1999).
- Dunbar, N. W., Zielinski, G. A. & Voisins, D. T. Tephra layers in the Siple Dome and Taylor Dome ice cores, Antarctica: Sources and correlations. *J. Geophys. Res.* **108**, 2374 (2003).
- Blong, R. J. *Volcanic Hazards A Sourcebook on the Effects of Eruptions* (Academic, 1984).
- Joughin, I., Tulaczyk, S., MacAyeal, D. R. & Engelhardt, H. Melting and freezing beneath the Ross ice streams, Antarctica. *J. Glaciol.* **50**, 96–108 (2004).
- Young, D. A. *et al.* A dynamic early East Antarctic Ice Sheet suggested by ice-covered fjord landscapes. *Nature* **474**, 72–75 (2011).
- Peters, M. E. *et al.* Along-track focusing of airborne radar sounding data from West Antarctica for improving basal reflection analysis and layer detection. *Geosci. Remote Sensing, IEEE Trans.* **45**, 2725–2736 (2007).
- Jordan, T. H. & Sverdrup, K. A. Teleseismic location techniques and their application to earthquake clusters in the south-central Pacific. *Bull. Seismol. Soc. Am.* **71**, 1105–1130 (1981).
- Scambos, T., Haran, T., Fahnestock, M., Painter, T. & Bohlander, J. MODIS-based Mosaic of Antarctica (MOA) data sets: Continent-wide surface morphology and snow grain size. *Remote Sens. Environ.* **111**, 242–257 (2007).

Acknowledgements

POLENET-Antarctica is supported by NSF Office of Polar Programs grant numbers 0632230, 0632239, 0652322, 0632335, 0632136, 0632209 and 0632185. GIMBLE is supported by NSF grant 1043761. Seismic instrumentation provided and supported by the Incorporated Research Institutions for Seismology (IRIS) through the PASSCAL Instrument Center at New Mexico Tech. Seismic data are available through the IRIS Data Management Center. The facilities of the IRIS Consortium are supported by the NSF under Cooperative Agreement EAR-1063471, the NSF Office of Polar Programs and the DOE National Nuclear Security Administration. This is UTIG contribution 2589.

Author contributions

A.C.L. carried out initial locations and relative relocations on all DLP events used and carried out statistical and spectral analysis on DLP events. C.G.B. reviewed automatic detection locations and located all non-DLP events. R.C.A. carried out waveform cross-correlations. D.A.Y. and D.D.B. reviewed all radar and magnetics data and provided radar profiles shown in the figures. All authors contributed comments to the interpretation of results and preparation of the final paper.

Additional information

Supplementary information is available in the [online version of the paper](#). Reprints and permissions information is available online at www.nature.com/reprints. Correspondence and requests for materials should be addressed to A.C.L.

Competing financial interests

The authors declare no competing financial interests.